Human Heart Segmentation Based on Differential Evolution and Active Contours with Shape Prior

Ivan Cruz-Aceves, Juan Gabriel Avina-Cervantes,
Juan Manuel Lopez-Hernandez, Ma. De Guadalupe Garcia-Hernandez,
Sheila Esmeralda Gonzalez-Reyna, and Miguel Torres-Cisneros

Universidad de Guanajuato, División de Ingenierías Campus Irapuato-Salamanca,
Carretera Salamanca-Valle de Santiago Km 3.5+1.8 Km Comunidad de Palo Blanco,
C.P. 36885 Salamanca, Gto., México
{i.cruzaceves,avina,jmlopez,garciag,se.gonzalezreyna,mtorres}@ugto.mx

Abstract. Active contour model is an image segmentation technique that uses the evaluation of internal and external forces to be attracted towards the edge of a target object. In this paper a novel image segmentation method based on differential evolution and active contours with shape prior is introduced. In the proposed method, the initial active contours have been generated through an alignment process of reference shape priors, and differential evolution is used to perform the segmentation task over a polar coordinate system. This method is applied in the segmentation of the human heart from datasets of Computed Tomography images. To assess the segmentation results compared to those outlined by experts and by different segmentation techniques, a set of similarity measures has been adopted. The experimental results suggest that by using differential evolution, the proposed method outperforms the classical active contour model and the interactive Tseng method in terms of efficiency and segmentation accuracy.

Keywords: Active Contour Model, Differential Evolution, Human Heart, Image Segmentation, Shape prior.

1 Introduction

In clinical practice the Computed Tomography (CT) scanning is an effective method for the monitoring and diagnosis of cardiac disease. The process carried out by cardiologists can be subjective and time-consuming because it is based on a visual examination followed by a manual delineation of the human organ. Due to this, the application of automatic image segmentation methods plays an important and challenging role.

In recent years, numerous approaches have been introduced for the automatic medical image segmentation such as, region growing in pelvic injuries [1], templates for atlas in radiotherapy [2], watershed transform for tumors in mammograms [3], and active contour model in mammographic images [4] and human

F. Castro, A. Gelbukh, M.G. Mendoza (Eds.): MICAI 2013, Part I, LNAI 8265, pp. 506–517, 2013.

prostate [5]. The active contour models (ACM) was introduced by [6] and it consists of an energy-minimizing spline composed of control points also called snaxels. This spline evolves through time according to the shape of a target object by evaluating internal and external forces. The traditional ACM implementation presents two shortcomings, firstly, the initialization of snaxels must be close to the target object, otherwise, failure of convergence will occur and, secondly, ACM is prone to be trapped into local minima because of the presence of noise. To solve these shortcomings some improvements have been suggested to adapt different methods working together with ACM including graph cut [7], statistical methods [8], population-based methods such as genetic algorithms [9,10] and particle swarm optimization (PSO) [11,12]. The performance of the ACM with population-based methods is suitable since the ACM becomes more robust, stable and efficient in the local minima problem.

Differential Evolution (DE) is a population-based method proposed by [13,14] similar to evolutionary algorithms. DE has become very popular to solve optimization problems with nonlinear functions with low computational time. In the classical implementation, the efficiency of the obtained results directly depends of three main parameters such as population size, differentiation factor and crossover rate. As DE is easy to implement, not computationally expensive and robust in the presence of noise, it has been used in many real-world applications including text summarization [15], job shop scheduling problem [16] and parameter estimation for a human immunodeficiency virus (HIV) [17].

In this paper, we introduce a novel image segmentation framework based on the theory of Active Contour Models with shape prior and Differential Evolution. The proposed framework is an adaptation of [18], here we use DE instead PSO to perform the optimization task increasing the exploitation capability regarding the classical Active Contour Model and the interactive Tseng method. Additionally, this framework uses the alignment process proposed in [19] to obtain an initial shape contour of the target object, which is scaled to different size to generate potential solutions. This proposed framework is applied in the segmentation of the human heart on Computed Tomography images from different patients, and the segmentation results are evaluated according to different similarity measures with respect to regions outlined by experts.

The paper is organized as follows. In Section 2, the fundamentals of the classical implementation of ACM and Differential Evolution are introduced. In Section 3 the proposed image segmentation framework is presented, along with a set of similarity measures. The experimental results are discussed in Section 4, and from the similarity analysis conclusions are given in Section 5.

2 Background

In this section, the fundamentals of the Active Contour Model and Differential Evolution optimization method are described in detail.

2.1 Active Contour Models

The traditional Active Contour Model (ACM) is a parametric curve that can move within a spatial image domain where it was assigned [6]. This curve is defined by $p(s,t) = (x(s,t), y(s,t)), s \in [0,1]$, where it evolves through time t to minimize the total energy function given by the following:

$$E_{snake} = \int_0^1 [E_{int}(p(s,t)) + E_{ext}(p(s,t))]\mathrm{d}s \tag{1}$$

This energy function consists of two energies, the internal energy E_{int} to maintain the search within the spatial image domain and to control the shape modification of the curve, and the external energy E_{ext}, which is defined by the particular gradient features of the image. On the other hand, the computational implementation of the traditional ACM uses a set of n discrete points $\{p_i | i = 1, 2, \ldots, n\}$, and the energy function is given by (2), which evaluates the actual control point to minimize the k_i index in the W_i searching window using (3).

$$E_{i,j} = E_{int} + E_{ext} \tag{2}$$

$$E_{snake} = \sum_{i=1}^{n} E_{i,k_i}, \;\; k_i = \arg\min_j(E_{i,j}), j \in W_i \tag{3}$$

Because of the traditional ACM presents the drawbacks of initialization and local minima, Chan & Vese [20] proposed the integration of a shape prior constraint within the traditional ACM. This method is given by the following:

$$E_T = w_1 E_1 + w_2 E_2 + w_3 E_3 \tag{4}$$

where E_T is the total energy function composed of the energies E_1, E_2, E_3 and their weighting factors w_1, w_2, w_3. E_1 represents the active contour, E_2 is the shape energy defined as the difference between the active contour and the shape template expressed as follows:

$$E_2 = \int_\Omega \left(H(\phi) - H(\varphi_T(B^T))\right)^2 dxdy \tag{5}$$

where Ω represents the image domain, $H(\cdot)$ is the Heaviside function, ϕ is the signed distance function, φ_T is the deformed template and B^T is the transformation matrix consisting of translation $[t_x, t_y]^T$ in the horizontal and vertical axes, the scaling factor $[s]$ and the rotation angle parameter $[\theta]$, as follows:

$$B^T = \underbrace{\begin{bmatrix} 1 & 0 & t_x \\ 0 & 1 & t_y \\ 0 & 0 & 1 \end{bmatrix}}_{M(a,b)} \times \underbrace{\begin{bmatrix} s & 0 & 0 \\ 0 & s & 0 \\ 0 & 0 & 1 \end{bmatrix}}_{H(s)} \times \underbrace{\begin{bmatrix} cos\theta & -sin\theta & 0 \\ sin\theta & cos\theta & 0 \\ 0 & 0 & 1 \end{bmatrix}}_{R(\theta)} \tag{6}$$

Finally, the energy E_3 represents the image-based force with an image intensity I and the gradient operator ∇ calculated as follows:

$$E_3 = \int_{\Omega} (\nabla H(\phi) - \nabla I)^2 dxdy \tag{7}$$

The three energies are iteratively evaluated until the difference between the previous and actual segmented object becomes stable. Although the initialization drawback of the traditional ACM is solved through the Chan & Vese method, this method remains prone to be trapped into local minima. A suitable alternative to overcome this drawback is to use population-based methods such as Differential Evolution, which is described in the following Section.

2.2 Differential Evolution

Differential evolution is a stochastic real-parameter method proposed by [13,14] to solve numerical global optimization problems. DE consists of a set of potential solutions, called individuals $X = \{x_1, x_2, \ldots, x_{Np}\}$, where Np is the population size. The individuals are iteratively improved by using different variation operators, and the solution is chosen to be the individual with the best fitness according to an objective function.

The main idea of the DE method consists of the mutation, crossover and selection operators based on the floating-point encoding. The mutation operator is used to create a mutant vector $V_{i,g+1}$ at each generation g based on the distribution of the current population $\{X_{i,g}|i = 1, 2, \ldots, Np\}$ through the following strategy,

$$V_{i,g+1} = X_{r1,g} + F(X_{r2,g} - X_{r3,g}), \quad r1 \neq r2 \neq r3 \neq i \tag{8}$$

where F is the differentiation factor, and $r1$, $r2$ and $r3$ represent the indexes of three different individuals and uniformly selected from the set {1,. . . ,Np}. The second operator is the crossover, which uses (9) to create the trial vector $U_{i,g+1}$ as follows:

$$U_{i,g+1} = \begin{cases} V_{i,g+1}, & \text{if } r \leq CR \\ X_{i,g} \quad , & \text{if } r > CR \end{cases} \tag{9}$$

where r represents a uniform random value on the interval $[0, 1]$, which is compared with the CR (crossover rate) parameter. If r is bigger than CR, the current information of individual $X_{i,g}$ is preserved, otherwise the information from the mutant vector $V_{i,g+1}$ is copied to the trial vector $U_{i,g+1}$. Subsequently, the selection procedure is applied by using (10). This procedure selects according to a fitness function, the better one between the trial vector $U_{i,g+1}$ and the current individual $X_{i,g}$.

$$X_{i,g+1} = \begin{cases} U_{i,g+1}, & \text{if } f(U_{i,g+1}) < f(X_{i,g}) \\ X_{i,g} \quad , & \text{otherwise} \end{cases} \tag{10}$$

According to the previous description, the traditional DE method is described below.

1. Initialize number of generations G, population size Np, value of differentiation factor F, and value of crossover rate CR.
2. Initialize each individual X_i.
3. For each individual $X_{i,g}$, where $g = \{1, \ldots, G\}$:
   (a) Calculate $V_{i,g+1}$ by using the mutation step (8).
   (b) Assign $U_{i,g+1}$ according to the crossover operator (9).
   (c) Update $X_{i,g+1}$, if $U_{i,g+1}$ is better than $X_{i,g}$ by applying the selection step (10).
4. Stop if the convergence criterion is satisfied (e.g., stability or number of generations).

3 Proposed Image Segmentation Framework

The proposed framework based on the theory of Active Contour Models and Differential Evolution is described in Section 3.1. Moreover, to evaluate the performance of the segmentation results, the Jaccard and Dice indexes are introduced in Section 3.2.

3.1 Scaled Active Contours Driven by Differential Evolution

Because of the disadvantages of the classical active contour model discussed above, Differential Evolution and scaled templates have been adopted. These templates are acquired from an alignment process of reference images to overcome the initialization drawback and DE is used to solve the local minima problem. Since the methodology of the proposed framework allows directly apply the optimization method in the segmentation problem, the advantages of robustness, efficiency and low computational time are inherently preserved. In Figure 1 the segmentation process performed by the proposed framework is described below.

The proposed framework consists on three steps. Firstly, the construction of a shape template by using an alignment process of a set of reference images is required. This alignment process consists in the estimation of the parameters $[a, b, s, \theta]^T$ according to [19] as follows:

$$\begin{bmatrix} \tilde{x} \\ \tilde{y} \\ 1 \end{bmatrix} = M(a,b) \times H(s) \times R(\theta) \times \begin{bmatrix} x \\ y \\ 1 \end{bmatrix} \tag{11}$$

where $M(a, b)$ represents the translation matrix on the horizontal x and vertical y axes, $H(s)$ is the scale matrix and $R(\theta)$ is the rotation matrix. The product of these matrices is used to apply the gradient descent method in order to minimize the following energy function:

$$E_{alig} = \sum_{i=1}^{n} \sum_{j=1, j\neq i}^{n} \left\{ \frac{\int\int_{\Omega} (\tilde{I}^i - \tilde{I}^j)^2 dA}{\int\int_{\Omega} (\tilde{I}^i + \tilde{I}^j)^2 dA} \right\} \tag{12}$$

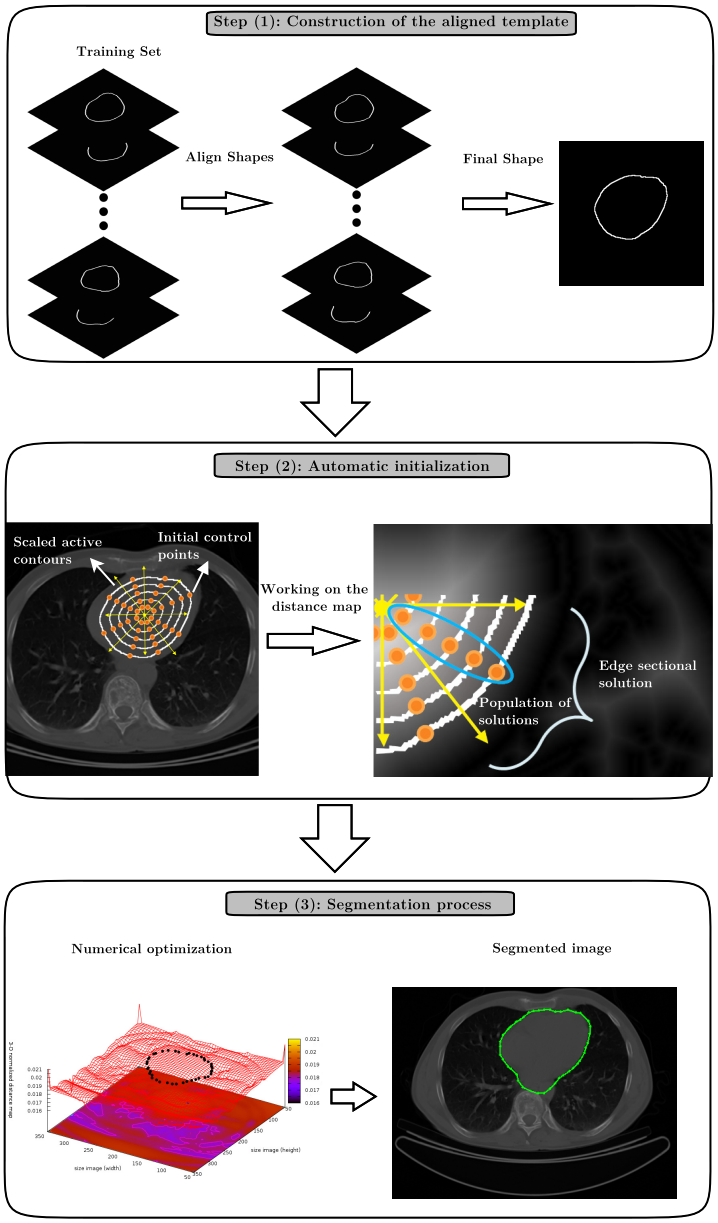

Fig. 1. Process of the proposed image segmentation method

where Ω represents the image domain and $\tilde{I}$ represents the transformed image. The final procedure in this step involves obtaining the final shape template, which is acquired through the maximum shape boundary from the whole set of superimposed transformed images.

Secondly, a preprocessing stage is performed. We use a 2D median filter (3×3 window size) to remove the noise from image. Then, the Canny edge detector is applied with the parameters $\sigma = 1.3$, $T_l = 10.0$ and $T_h = 30.0$ experimentally tuned to preserve the real edges of the human heart from the background image. Subsequently, the Euclidean distance map (EDM) [21] is computed as potential surface to perform the optimization task. The EDM assigns high potential values to image pixels located far from the human heart, and low potential values (ideally zero) to pixels located close to the heart. On the resulting EDM, the automatic initialization process is performed through the maximum mutual information between the final template and the current test image. The n initial scaled active contours are generated by scaling the final template from the previous alignment process. The number of scaled active contours has to be considered assuming that the human heart is confined within them. These scaled contours must be discretized by a number m of control points to smooth and adapt the resulting contour to the shape of the target object.

To perform the optimization process, the control points are assigned as individuals to conform m populations P. Each population is composed of control points of different contours with the same position label. The final step of the proposed framework consists on the numerical optimization followed by the image segmentation result. The numerical optimization is performed on the Euclidean distance map (range [0,255]), which represents the fitness function in the optimization process. Differential Evolution is applied for each population P_i separately in order to minimize the nearest edge sectional solution. If the DE strategy for each population P_i is finished, the final segmentation result is acquired by connecting the best individual of each population to each other.

The proposed image segmentation framework can be implemented by using the following procedure:

1. Align reference images according to [19] and obtain final template.
2. Perform maximum mutual information to positioning the final template.
3. Initialize parameter n of scaled active contours and parameter m of control points.
4. Initialize the DE parameters: generations, differentiation factor and crossover rate.
5. Generate m populations assigning the control points as individuals.
6. For each population P_i:
   (a) Apply restriction of the search space to ignore improper solutions.
   (b) Evaluate each individual in fitness function (EDM).
   (c) Calculate $V_{i,g+1}$ by using the mutation step (8).
   (d) Assign $U_{i,g+1}$ according to the crossover operator (9).
   (e) Update $X_{i,g+1}$, if $U_{i,g+1}$ is better than $X_{i,g}$ by applying the selection step (10).
7. Stop if the convergence criterion is satisfied (e.g., stability or number of generations).

3.2 Validation Metrics

To assess the performance of the proposed framework on medical images, Jaccard and Dice indexes have been adopted to analyze the segmentation results between the regions outlined by experts and the regions obtained by computational methods.

The Jaccard $J(A, B)$ and Dice $D(A, B)$ indexes are similarity measures used for binary variables [3], which are defined in the range $[0, 1]$ and they are computed using (13) and (14), respectively. In our tests, A represents the regions outlined by experts (ground truth) and B represents the automatic segmented region by computational methods.

$$J(A, B) = \frac{A \cap B}{A \cup B} \tag{13}$$

$$D(A, B) = \frac{2(A \cap B)}{A + B} \tag{14}$$

In these indexes, if the regions A and B are completely superimposed the obtained result is 1.0, otherwise, if these two regions are completely different the obtained result is 0.

In Section 4, the segmentation results obtained from the proposed framework on computed tomography images are analyzed by the similarity metrics.

4 Experimental Results

In this section, the proposed image segmentation framework is applied for segmenting the human heart in Computed Tomography images. The computational simulations are performed with an Intel Core i3 with 4Gb of memory and 2.13Ghz using the GNU Compiler Collection (C++) version 4.4.5.

In Figure 2(a) a CT image of the human chest is illustrated, in order to have better understanding of the segmentation task. Figure 2(b) shows the resulting Euclidean distance map of the test image, in which the optimization process is applied. In Figures 2(c) and (d) the human heart outlined by expert 1 and expert 2 are presented to have reference ground truth for the experiments with the proposed methodology.

In Figure 3 the human heart segmentation results on a subset of Computed Tomography images are introduced. The whole dataset is composed of 144 CT images with size 512×512 pixels from different patients. In Figure 3(a) the manual delineations of the human heart made by cardiologists are presented. Figure 3(b) illustrates the segmentation results obtained via the traditional implementation of Active Contour Model, where the fitting problem and local minima problem are clearly shown. The ACM parameters were set according to [11] as 45 control points, $\alpha = 0.017$, $\beta = 0.86$ and $\gamma = 0.45$, obtaining an average execution time of 0.172s per image. Figure 3(c) presents the segmentation results obtained through the interactive Tseng method, in which, each control point is provided interactively by the user. The parameters of this implementation were

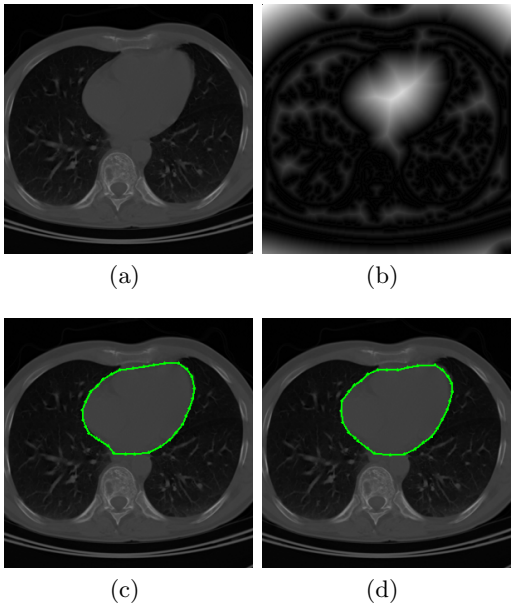

Fig. 2. CT image: (a) test image, (b) Euclidean distance map of test image, (c) human heart outlined by expert 1 and (d) human heart outlined by expert 2

set as 45 control points, window size 30×30 pixels, and for each control point 9 particles are created, given an average execution time of 0.214s per image. Even though the use of a square matrix in the Tseng method obtained suitable segmentation results, this method presents problems to fit the real human heart boundary accurately. Finally, in Figure 3(d) the segmentation results obtained by using the proposed segmentation framework presents an appropriate human heart segmentation. This method avoid the local minima and it fits the human heart accurately with parameters set as number of scaled contours = 9, number of control points = 45, iterations = 10, crossover rate = 0.9, and the differentiation factor = 0.5, obtaining an average execution time of 0.223s per image. The differentiation factor was experimentally tuned to perform local exploitation and reduce the number of improper solutions.

From the aforementioned dataset of CT images, in Table 1 the average of the segmentation results obtained by the classical ACM, interactive Tseng method and our proposed framework is compared to those regions delineated by cardiologists. The similarity results suggest that the proposed method can lead to more efficiency in human heart segmentation with respect to the comparative methods, which can significantly help cardiologists in clinical practice. The quality of the human heart segmentation results obtained with the proposed framework depends on parameter selection. We used a experimentally tuned value as differentiation factor to perform local exploitation, and the constant parameters in our experiments are suitable for other images, since the DE method is directly applied to minimize one edge sectional solution for each polar area.

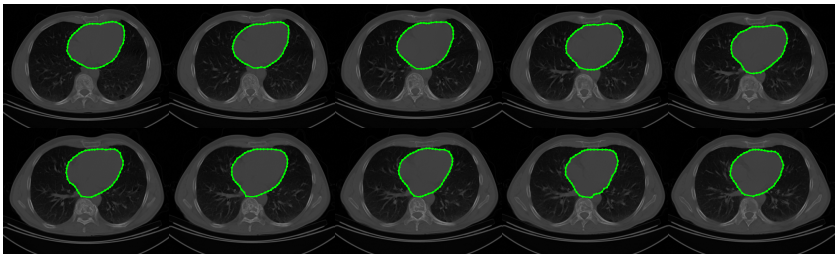

(a)

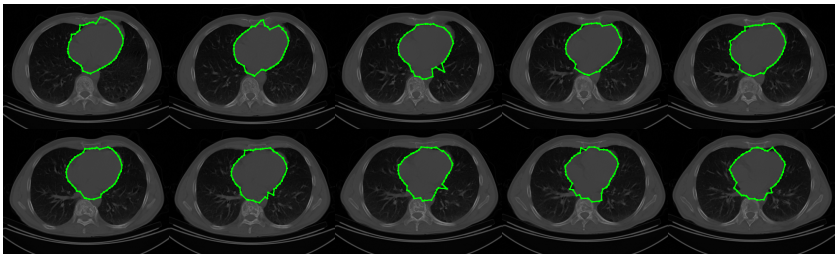

(b)

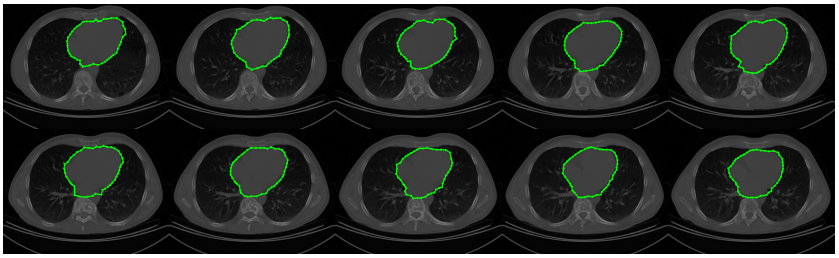

(c)

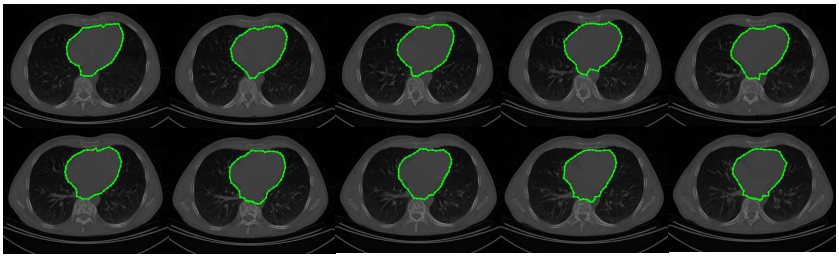

(d)

Fig. 3. CT images (human heart segmentation): (a) manual delineation by experts, (b) results of traditional ACM, (c) results of interactive Tseng method and (d) results of proposed implementation

Table 1. Average similarity measure with the Jaccard and Dice indexes among the human heart segmented by the traditional ACM, interactive Tseng method, our proposed method, and the regions outlined by experts of the CT dataset

Comparative Studies	Similarity Measure	
	Jaccard index *(J)*	**Dice index *(D)***
ACM vs Experts	0.6666	0.8000
Tseng vs Experts	0.8000	0.8888
Proposed method vs Experts	0.8367	0.9111

5 Conclusions

In this paper, a novel image segmentation framework based on the theory of active contour models with shape prior and differential evolution has been introduced. The proposed framework uses an alignment process to generate different scaled contours according to the shape of the target object. Subsequently, differential evolution is used to perform the segmentation task within constrained polar sections. This novel framework was used to segment the human heart from Computed Tomography images allowing to overcome the local minima problem and the sensitivity to initial position regarding the comparative methods. To assess the segmentation results obtained through the proposed framework, Jaccard and Dice indexes were used. According to the experimental results, the proposed framework is suitable to the human heart segmentation, since the exploitation capability of differential evolution is efficient to overcome the local minima problem to fit the heart boundary accurately.

Acknowledgments. This research has been supported by the National Council of Science and Technology of México (CONACYT) under Grant 241224-218157. The authors thanks "Programa Integral de Fortalecimiento Institucional 2012 (PIFI-2012)" for financial support and at the cardiology deparment of the Mexican Social Security Institute UMAE T1 Leon, for clinical advice and for kindly providing us the sources of CT images.

References

1. Davuluri, P., Wu, J., Tang, Y., et al.: Hemorrhage detection and segmentation in traumatic pelvic injuries. Computational and Mathematical Methods in Medicine 2012, 12 (2012)
2. Parraga, A., Macq, B., Craene, M.: Anatomical atlas in the context of head and neck radiotherapy and its use to automatic segmentation. Biomedical Signal Processing and Control, 447–455 (2012)
3. Hsu, W.: Improved watershed transform for tumor segmentation: Application to mammogram image compresion. Expert Systems with Applications 39, 3950–3955 (2012)
4. Jumaat, A., Rahman, W., Ibrahim, A., Mahmud, R.: Segmentation of masses from breast ultrasound images using parametric active contour algorithm. Procedia Social and Behavioral Sciences 8, 640–647 (2010)

5. Liu, X., Haider, M., Yetik, I.: Unsupervised 3d prostate segmentation based on diffusion-weighted imaging mri using active contour models with a shape prior. Journal of Electrical and Computer Engineering, 11 (2011)
6. Kass, M., Terzopoulos, A.W.D.: Snakes: Active contour models. International Journal of Computer Vision 1, 321–331 (1988)
7. Cheng, Y., Wang, Z., Hu, J., Zhao, W., Wu, Q.: The domain knowledge based graph-cut model for liver ct segmentation. Biomedical Signal Processing and Control 7, 591–598 (2012)
8. Wang, L., He, L., Mishra, A., Li, C.: Active contours driven by local gaussian distribution fitting energy. Signal Processing 89, 2435–2447 (2009)
9. Ballerini, L.: Genetic snakes for medical images segmentation. In: Poli, R., Voigt, H.-M., Cagnoni, S., Corne, D.W., Smith, G.D., Fogarty, T.C. (eds.) EvoIASP 1999 and EuroEcTel 1999. LNCS, vol. 1596, pp. 59–73. Springer, Heidelberg (1999)
10. Talebi, M., Ayatollahi, A., Kermani, A.: Medical ultrasound image segmentation using genetic active contour. Journal of Biomedical Science and Engineering 4, 105–109 (2011)
11. Tseng, C., Hiseh, J., Jeng, J.: Active contour model via multi-population particle swarm optimization. Expert Systems with Applications 36, 5348–5352 (2009)
12. Shahamatnia, E., Ebadzadeh, M.: Application of particle swarm optimization and snake model hybrid on medical imaging. In: Proceedings of the Third International Workshop on Computational Intelligence in Medical Imaging, pp. 1–8 (2011)
13. Storn, R., Price, K.: Differential evolution - a simple and efficient adaptive scheme for global optimization over continuous spaces. Technical Report TR-95-012, International Computer Sciences Institute, Berkeley, CA, USA (1995)
14. Storn, R., Price, K.: Differential evolution – a simple and efficient heuristic for global optimization over continuous spaces. Journal of Global Optimization 11, 341–359 (1997)
15. Alguliev, R., Aliguliyev, R., Mehdiyev, C.: psum-sade: A modified p-median problem and self-adaptive differential evolution algorithm for text summarization. Applied Computational Intelligence and Soft Computing 13 (2011)
16. Zhang, R., Wu, C.: A hybrid differential evolution and tree search algorithm for the job shop scheduling problem. Mathematical Problems in Engineering, 20 (2011)
17. Ho, W., Chan, A.: Hybrid taguchi-differential evolution algorithm for parameter estimation of differential equation models with application to hiv dynamics. Mathematical Problems in Engineering, 14 (2011)
18. Cruz-Aceves, I., Avina-Cervantes, J., Lopez-Hernandez, J., et al.: Unsupervised cardiac image segmentation via multi-swarm active contours with a shape prior. Computational and Mathematical Methods in Medicine, 15 (2013)
19. Tsai, A., Yezzi, A., Wells, W., Tempany, C., Tucker, D., Fan, A., Grimson, W., Willsky, A.: A shape-based approach to the segmentation of medical imagery using level sets. IEEE Transactions on Medical Imaging 22, 137–154 (2003)
20. Chan, T., Vese, L.: Active contours without edges. IEEE Transactions on Image Processing 10, 266–277 (2001)
21. Cohen, L., Cohen, I.: Finite-element methods for active contour models and balloons for 2-d and 3-d images. IEEE Transactions on Pattern Analysis and Machine Intelligence 15, 1131–1147 (1993)